J Eng Math (2008) 60:249–264
DOI 10.1007/s10665-007-9161-7

# Operating charts for continuous sedimentation IV: limitations for control of dynamic behaviour

**Stefan Diehl**

Received: 10 May 2007 / Accepted: 8 June 2007 / Published online: 25 July 2007


**Abstract** The nonlinear behaviour of a one-dimensional idealized model of continuous sedimentation has been investigated in this series of papers. The model is a scalar hyperbolic conservation law with a space-discontinuous flux function and a point source. Parameters in the equation are the two input variables (concentration and flux) and the control variable (a volume flow). The most desired type of solution contains a large concentration discontinuity and is referred to as 'optimal operation'. Operating charts (concentration-flux diagrams) have proved to be a means for classifying the nonlinear behaviour. In this paper, some fundamental results on the dynamic behaviour are presented, which give information on the limitations of the range of the control variable. When this is used together with the previously introduced optimal control strategies for step inputs, the process can be controlled.

**Keywords** Continuous sedimentation · Control · Dynamic behaviour · Operating chart · Thickener

## 1 Introduction

The aim of the process of continuous sedimentation is to separate particles from a liquid in a large tank under a continuous inflow of mixture at an intermediate feed level. The particles settle by gravitation and are also influenced by a bulk flow upwards above the feed inlet (the clarification zone), and a bulk flow downwards below the feed inlet (the thickening zone), see Fig. 1 (left). Under optimal operating conditions, there is a discharge of a highly concentrated suspension at the bottom (the underflow) simultaneously with a clarified overflow of liquid at the top of the tank (the effluent). The continuous-sedimentation tank is widely used in mineral processing, wastewater-treatment plants, chemical engineering etc., and is called *clarifier–thickener unit*, gravity thickener, gravity settler, secondary clarifier, or just *settler*. Under optimal operating conditions there are no particles in the clarification zone and there is a large concentration discontinuity in the thickening zone, called the *sludge blanket* in wastewater treatment. This state of the settler is called *optimal operation*.

Even under idealized assumptions, such as, all flows in the tank occur only in one dimension, the cross-sectional area is constant, the feed inlet is a point source, and the particles are equally-sized spheres that form a incompressible sediment at a maximum concentration, the process is still highly nonlinear because of the feed source, the outlets and the settling properties.

S. Diehl (✉)
Centre for Mathematical Sciences, Lund University, P.O. Box 118, 221 00 Lund, Sweden
e-mail: diehl@maths.lth.se

The process has been used for about a century. The need for information to the operators of the plants has led to the 'engineering' development of rules, operating charts and graphical tools based on experiments and physical considerations in parallel to the development of mathematically rigorous descriptions of the process by partial differential equations (PDEs). In both of these two parallel developments, the idealized assumptions described above have been the most common.

The aim of the present series of papers (the previous ones are [1–3]) is to give a deeper knowledge of the behaviour of an idealized one-dimensional clarifier–thickener model for all possible input data and to present the possibilities and limitations of control. The hyperbolic PDE model was formulated and analysed in [4,5], in which existence and uniqueness locally in time were proved. Global existence and uniqueness were established by Bürger et al. [6,7] and Karlsen and Towers [8].

The PDE model is hyperbolic because of the constitutive assumption by Kynch [9]: the settling flux of particles is a function only of the concentration. This has also been the basis for the parallel 'engineering' development without PDEs. References, discussions and developments relating to concepts such as the 'solids-flux theory', operating charts etc. can be found in [1]. We mention here only the papers by Keinath, Laquidara et al. [10–12], which contain interpretations concerning clarification failure and control related to the results of the present paper. References relating to the development of PDE models and numerical algorithms can be found in [2].

In particular, the important contribution by Bürger et al. [13], which relies on the analyses by Karlsen et al. [14,15], contains a generalization of the previous results (existence, uniqueness and numerical method) for the hyperbolic equation to the case when also compression at high concentrations is modelled, which leads to a strongly degenerate parabolic PDE. Many suspensions exhibit sediment compressibility for high concentrations. It is, however, not possible to construct analytical dynamic solutions for the degenerate parabolic model in contrast to the hyperbolic one. Because of this, and several other reasons discussed in [1,2], this series of papers deals with the simpler hyperbolic model for suspensions forming incompressible sediments. Another reason is that a systematic analysis of the possibilities and limitations for controlling the process cannot be found in the literature. Analyses, based on PDE solutions, of control possibilities under normal operating conditions can be found in [16–22].

The need to control the settler is emphasized in several applications, see e.g. [12,23–42]. In particular, the diurnal periodic load to wastewater treatment plants are of major concern, as well as the additional transient complications caused by, for example, storm events; see the numerical simulations, experimental data and discussions in, for example, [43–52].

During long periods of periodically varying feed concentration and associated flux with small oscillations and with constant mean values, the settler is approximately in steady state and there may be no need for any control action. If the amplitudes of the oscillations grow, when is a control action required in order to maintain optimal operation? What is a good value of the control variable? In the present paper we answer the first question and illustrate the problems of finding an answer to the second. The second question will be answered in [53] by means of a regulator, which is partly based on the result in the present paper.

In this series of papers, the nonlinear behaviour has been investigated thoroughly in terms of solutions of the hyperbolic PDE. In classifying the qualitatively different behaviours, a useful means is the engineering concept of '*operating chart*'; a concentration-flux diagram that is divided into several regions depending on the batch-settling flux function, the value of the control variable, etc. For all possible locations of the *feed point* (input concentration and flux) in such a chart, the possible steady states have been classified in [1]. Several relations between interesting variables (control variable, outputs, maximum thickening factor, etc.) and the feed point were also given for steady-state solutions. In [2], the state of *optimal operation* was defined as a special type of dynamic solution. Furthermore, all qualitatively different step responses were classified in the case when the settler is in optimal operation initially and the control variable (the volume underflow rate) is held constant. The same initial conditions and step inputs were used in [3], and the control variable was adjusted according to optimal control strategies in order to meet different suggested control objectives.

In the present paper we investigate and give rules on how to control the process during dynamic operation, i.e., as the feed point moves around in the operating chart. We focus on the main condition of the previously presented control objectives: to maintain optimal operation as long as possible. In Sect. 2, the process, the model and the previous results are reviewed briefly. In Sect. 3, some fundamental results on the solution of the PDE are presented. These yield information on the limitations of the control variable's range. Since we can control step inputs, see [3], a natural next step is to investigate how to control periodic inputs consisting of a series of steps. This is done in Sect. 4. Such discontinuous inputs, with large oscillations, are believed to be of the worst-case type, since the input variables in reality are usually continuous with respect to time.

## 2 Preliminaries

In order to investigate explicit solutions of the present problem with such nonlinear features it is necessary to use a comprehensive set of notation. Here, we review only briefly the fundamental notation and results presented in the preceding papers [1–3]. These concepts are sufficient for understanding the ideas, results and simulations of the paper. In the proofs of the theorems, and some discussions in Sect. 3, the full notation and assumptions on the construction of solutions will be used without further reference.

### 2.1 The clarifier–thickener unit and the model

The one-dimensional model of the clarifier–thickener unit, or settler, was first presented in [5]. The full notation for constructing solutions are given in [2, Sect. 2], to which we refer the reader.

Figure 1 shows the settler and the flux function in the thickening zone for three different values of the control parameter $Q_{\mathrm{u}}$. The purposes of the settler may vary depending on in what industrial process it is involved. At least in wastewater treatment the main *purposes* of the settler are the following. It should

1. produce a low effluent concentration;
2. produce a high underflow concentration;
3. work as a buffer of mass and be insensitive to small variations in the feed variables.

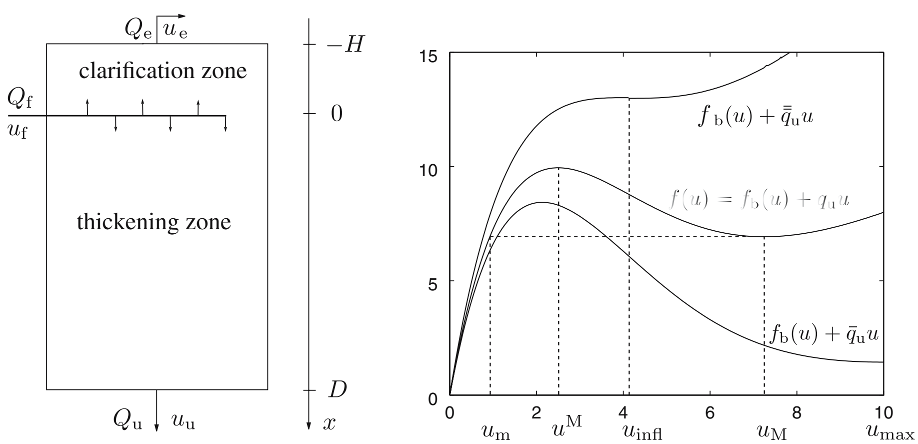


**Fig. 1** *Left*: Schematic picture of an ideal one-dimensional clarifier–thickener unit, where $u$ stands for concentration and $Q$ for volume flow of the feed, effluent and underflow streams, respectively. The flow restrictions are $Q_{\mathrm{f}} = Q_{\mathrm{e}} + Q_{\mathrm{u}} > 0$ and $Q_{\mathrm{e}} \geq 0$. For the numerical simulations we use $H = 1\,\mathrm{m}$, $D = 4\,\mathrm{m}$, and $A = \pi 30^2\,\mathrm{m}^2 \approx 2827\,\mathrm{m}^2$ for the constant cross-sectional area. *Right*: Flux curves $f(u)$ in the thickening zone and characteristic concentrations. The bulk velocities are defined as $q_{\mathrm{e}} = Q_{\mathrm{e}}/A$ etc. The constant $u_{\mathrm{infl}}$ is the inflection point of $f_{\mathrm{b}}(u)$ and $f(u) = f_{\mathrm{b}}(u) + q_{\mathrm{u}} u$. For $\bar{q}_{\mathrm{u}} < q_{\mathrm{u}} < \bar{\bar{q}}_{\mathrm{u}}$ there is a local minimum point $u_{\mathrm{M}}$ of $f(u)$ that lies between $u_{\mathrm{infl}}$ and $u_{\mathrm{max}}$. Given $u_{\mathrm{M}}$, $u_{\mathrm{m}}$ is the lower concentration defined by $f(u_{\mathrm{m}}) = f(u_{\mathrm{M}})$. For $q_{\mathrm{u}} < \bar{\bar{q}}_{\mathrm{u}}$ there is a local maximum point, $u^{\mathrm{M}}$ ($< u_{\mathrm{infl}}$) of $f(u)$. The batch-settling flux used for demonstrations with numerical simulations is $f_{\mathrm{b}}(u) = 10u\left((1 - 0.64u/u_{\mathrm{max}})^{6.55} - 0.36^{6.55}\right)\left[\mathrm{kg}/(\mathrm{m}^2\mathrm{h})\right]$

The one-dimensional model of the settler is the following. The conservation law can be written as the partial differential equation

$$u_t + (F(u,x,t))_x = s(t)\delta(x), \tag{1}$$

where $\delta$ is the Dirac measure, the total flux function is

$$F(u,x,t) = \begin{cases} -q_{\mathrm{e}}(t)u, & x < -H \\ g\left(u, Q_{\mathrm{e}}(t)\right) = f_{\mathrm{b}}(u) - q_{\mathrm{e}}(t)u, & -H < x < 0 \\ f\left(u, Q_{\mathrm{u}}(t)\right) = f_{\mathrm{b}}(u) + q_{\mathrm{u}}(t)u, & 0 < x < D \\ q_{\mathrm{u}}(t)u, & x > D, \end{cases}$$

and the source function is

$$s(t) = \frac{Q_{\mathrm{f}}(t)}{A}u_{\mathrm{f}}(t) = \frac{Q_{\mathrm{u}}(t) + Q_{\mathrm{e}}(t)}{A}u_{\mathrm{f}}(t) = \left(q_{\mathrm{u}}(t) + q_{\mathrm{e}}(t)\right)u_{\mathrm{f}}(t).$$

For convenience, the dependences of the flux functions within the settler on the (time varying) volume flows are often not written out, i.e., we write $g(u)$ and $f(u)$. The physical input variables are the feed concentration $u_{\mathrm{f}}$ and the feed volume flow $Q_{\mathrm{f}}$. For graphical interpretations in operating charts it is, however, convenient to use the *feed point* $(u_{\mathrm{f}}, s)$ as input variable. The *control variable* of the process is $Q_{\mathrm{u}}$ and has the natural restriction $0 < Q_{\mathrm{u}} \le Q_{\mathrm{f}}$. Two particular values of this variable arise from the properties of the batch settling flux function. Define

$$\bar{q}_{\mathrm{u}} = -f_{\mathrm{b}}'(u_{\max}), \qquad \bar{Q}_{\mathrm{u}} = \bar{q}_{\mathrm{u}}A,$$
$$\bar{\bar{q}}_{\mathrm{u}} = -f_{\mathrm{b}}'(u_{\mathrm{infl}}), \qquad \bar{\bar{Q}}_{\mathrm{u}} = \bar{\bar{q}}_{\mathrm{u}}A,$$

which are the bulk velocities such that the slope of $f$ is zero at $u_{\max}$ and $u_{\mathrm{infl}}$, respectively; see Fig. 1 (right).

## 2.2 Operating charts for control of steady states

Figure 2 shows the 'steady-state chart' and the 'control chart'. Depending on the location of the feed point $(u_{\mathrm{f}}, s)$ in the steady-state chart, there are different possible steady-state solutions, which are all piecewise constant and non-decreasing with depth; see [1, Table 1] for a complete table. The *limiting flux* is defined as:

$$f_{\lim}(u) = \min_{u \le \alpha \le u_{\max}} f(\alpha) = \begin{cases} f(u), & u \in [0, u_{\mathrm{m}}] \cup [u_{\mathrm{M}}, u_{\max}], \\ f(u_{\mathrm{M}}), & u \in (u_{\mathrm{m}}, u_{\mathrm{M}}); \end{cases}$$

see Fig. 2 (left). The graph of this function, together with pieces of straight lines, divides the operating chart into several regions (definitions are stated in [2]). The limiting flux, as well as the characteristic concentrations and the regions of the steady-state chart, depend on the control variable $Q_{\mathrm{u}}$; e.g. $u_{\mathrm{M}}(Q_{\mathrm{u}})$, $f(u, Q_{\mathrm{u}})$ and $f_{\lim}(u_{\mathrm{f}}, Q_{\mathrm{u}})$. The following regions in the operating chart are independent of $Q_{\mathrm{u}}$:

$$\Lambda_i = \bigcup_{Q_{\mathrm{u}}>0} \ell_i(Q_{\mathrm{u}}), \quad i = 1, \ldots, 4,$$

$$P = P_1 \cup P_2, \quad \text{where} \quad P_1 = \bigcup_{0<Q_{\mathrm{u}}\le\bar{\bar{Q}}_{\mathrm{u}}} p(Q_{\mathrm{u}}), \quad P_2 = \bigcup_{Q_{\mathrm{u}}>\bar{\bar{Q}}_{\mathrm{u}}} p(Q_{\mathrm{u}}),$$

$$\Lambda_{3\mathrm{a}} = \Lambda_3 \cap \left\{(u,y) : y < f_{\mathrm{b}}(u_{\mathrm{infl}}) + \bar{\bar{q}}_{\mathrm{u}}u_{\mathrm{infl}}\right\} \quad \text{and} \quad \Lambda_{3\mathrm{b}} = \Lambda_3 \backslash \Lambda_{3\mathrm{a}};$$

see Fig. 2 (right). Given a feed point in this chart, there is a unique graph $f_{\lim}(\cdot, \tilde{Q}_{\mathrm{u}})$ that passes through the feed point, see [1, Theorem 2]. With this unique value $\tilde{Q}_{\mathrm{u}}$ on the control parameter, the settler is critically loaded in steady state.

## 2.3 Optimal operation

The concept of *optimal operation in steady state* means that the concentration is zero in the clarification zone and there is a discontinuity in the thickening zone between the concentrations $u_{\mathrm{m}}$ and $u_{\mathrm{M}}$; see Fig. 1 (right). This

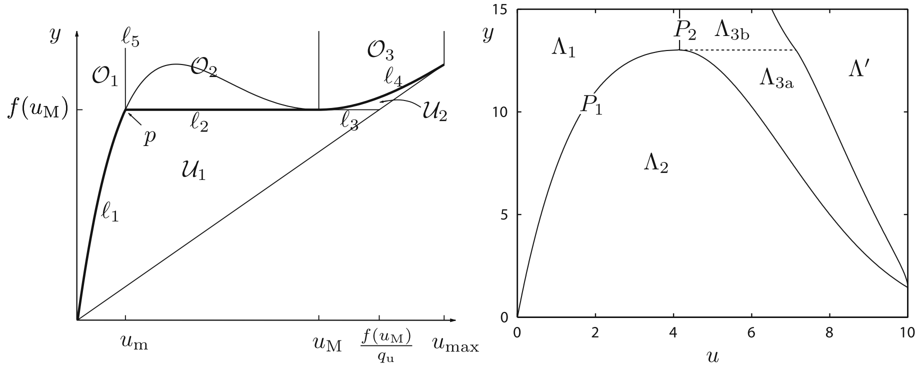


**Fig. 2** *Left:* The steady-state chart. The thick graph is the limiting flux curve. If the feed point lies on this curve, the settler is critically loaded in steady state, which means that it works at its maximum capacity. Below this graph the settler is underloaded, and above it is overloaded with a non-zero effluent concentration. Each region corresponds to a specific steady state which is unique, except on the limiting flux curve (and on $\ell_3$ and $\ell_5$), where the location of a discontinuity in the thickening and/or the clarification zone is not uniquely determined. Note that the regions in this chart all depend on $Q_{\rm u}$. *Right*: The control chart with respect to steady states; $\Lambda_3 = \Lambda_{3a} \cup \Lambda_{3b}$, $\Lambda_4 = \Lambda_3 \cup \Lambda'$. The regions in this chart are fixed (given the batch settling flux $f_{\rm b}$)

discontinuity is, in wastewater treatment, called the *sludge blanket* and its location at the depth $x = x_{\rm sb} \in (0, D)$ is called the sludge blanket level (SBL). A rising SBL refers to reality, although the $x$-coordinate decreases, because of the downward-pointing $x$-axis. A necessary condition for this state is that $(u_{\rm f}, s) \in p(Q_{\rm u}) \cup \ell_2(Q_{\rm u}) \cup \ell_3(Q_{\rm u})$ and $Q_{\rm u} < \bar{\bar{Q}}_{\rm u}$, which implies $(u_{\rm f}, s) \in P_1 \cup \Lambda_2 \cup \Lambda_{3a}$; see Fig. 2.

For a general dynamic solution, optimal operation and the SBL are defined as follows. Let $u_{\rm cl}$ denote the restriction of the solution $u$ to the clarification zone.

**Definition 2.1** The settler is said to be in *optimal operation* at time $t$ if $Q_{\rm u}(t) < \bar{\bar{Q}}_{\rm u}$ and the solution of (1) satisfies:

- $u_{\rm cl}(x, t) = 0 \Leftrightarrow u(x, t) = 0, -H < x < 0$,
- there exists a level $x_{\rm sb}(t) \in (0, D)$ such that

$$u(x, t) \in \begin{cases} [0, u_{\rm infl}), & 0 < x < x_{\rm sb}(t) \\ [u_{\rm infl}, u_{\rm max}], & x_{\rm sb}(t) < x < D. \end{cases}$$

The definition implies a natural definition of the SBL for a settler in optimal operation: it is the discontinuity at the level $x = x_{\rm sb}(t)$ in the thickening zone, such that the jump in the concentration passes the characteristic concentration $u_{\rm infl}$. It is convenient to use this definition of the SBL also when there are particles in the clarification zone.

## 2.4 Strategies for controlling step inputs

To satisfy the three purposes of the settler mentioned above, some *control objectives* for the process were introduced in [3, Table 1]. The main condition of these is to *maintain optimal operation as long as possible*. The objectives are exhaustive in the sense that they can always be met, also after optimal operation cannot be maintained (since the last condition, $u_{\rm e} = 0$, always can be satisfied).

Assume that the feed point $(u_{\rm f}(t), s(t))$ moves around, continuously and/or discontinuously, in the operating chart. To fulfil any control objective, *control strategies* need to be specified, which means that $Q_{\rm u}$ is defined as a function of the feed point and possibly the SBL. By a *control action* we mean a relation between $Q_{\rm u}$ and $(u_{\rm f}, s)$ at a fixed time point. In order to formulate control strategies we define the following subsets, or *lines*, in the operating chart:

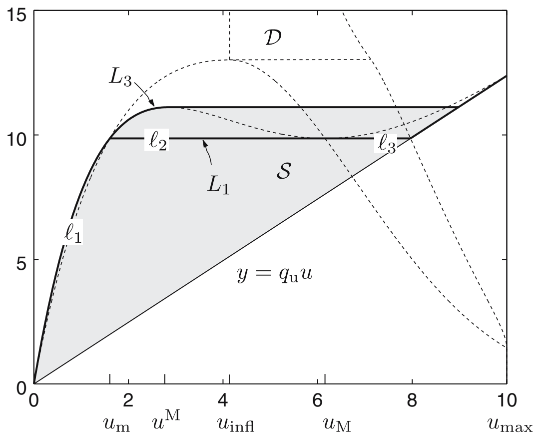


**Fig. 3** The lines $L_1$ and $L_3$, which coincide for low and high concentrations. The set $\mathcal{S}$ (the 'safe' region) is the closed region below $L_3$, shaded in the figure. $\mathcal{D}$ (the 'dangerous' region) is its complement, i.e. it lies strictly above $L_3$. (Note that the feed point has to lie on or above the line $y = q_{\mathrm{u}}u$, since $s = Q_{\mathrm{f}}u_{\mathrm{f}}/A \geq Q_{\mathrm{u}}u_{\mathrm{f}}/A = q_{\mathrm{u}}u_{\mathrm{f}}$.)

$$\begin{aligned}
L_1 &= \bigcup_{i=1}^{3} \ell_i \cup p \cup \left\{(u, y) : y = q_{\mathrm{u}}u,\ \frac{f(u_{\mathrm{M}})}{q_{\mathrm{u}}} < u \leq u_{\max}\right\}, \\
L_2 &= \left\{(u, y) : y = f_{\lim}(u)\right\} = \ell_1 \cup p \cup \ell_2 \cup \ell_4, \\
L_3 &= \left\{(u, y) : y = f_3(u)\right\} \quad \text{where } f_3(u) = \begin{cases} f(u), & 0 \leq u \leq u^{\mathrm{M}} \\ f(u^{\mathrm{M}}), & u^{\mathrm{M}} < u \leq \frac{f(u^{\mathrm{M}})}{q_{\mathrm{u}}} \\ q_{\mathrm{u}}u, & \frac{f(u^{\mathrm{M}})}{q_{\mathrm{u}}} < u \leq u_{\max}. \end{cases}
\end{aligned}$$

Note that these sets depend on $Q_{\mathrm{u}}$. For example, $(u_{\mathrm{f}}, s) \in L_2(Q_{\mathrm{u}})$ means that the feed point lies on the limiting flux (see Fig. 2, left) and the settler is critically loaded in the corresponding steady state. $L_1$ and $L_3$ are shown in Fig. 3. In this figure the following sets, which are used in Sect. 3, are also shown:

$$\mathcal{S} = \left\{(u, y) : q_{\mathrm{u}}u < y \leq f_3(u)\right\}, \qquad \mathcal{D} = \left\{(u, y) : 0 \leq u \leq u_{\max},\ y > f_3(u)\right\}.$$

By the *control strategy* DCL1 (direct control with respect to $L_1$) we mean that $Q_{\mathrm{u}}(t)$ is defined such that $(u_{\mathrm{f}}(t), s(t)) \in L_1(Q_{\mathrm{u}}(t))$. DCL2 and DCL3 are defined analogously. In all three strategies the value of $Q_{\mathrm{u}}$ is uniquely determined by the feed point $(u_{\mathrm{f}}, s)$. It is therefore convenient to use the notation $Q_{\mathrm{u}} = L_1^{-1}(u_{\mathrm{f}}, s) \Leftrightarrow (u_{\mathrm{f}}, s) \in L_1(Q_{\mathrm{u}})$ etc. Strategy DCL2 is motivated by the results on the control of steady states in [1]. Strategies DCL1 and DCL2 only differ for feed points in $(u_{\mathrm{f}}, s) \in \Lambda_3 \cup \Lambda'$, and in [3] we have seen that for step inputs DCL1 is more advantageous than DCL2.

## 3 Dynamic behaviour

For a settler initially in optimal operation in steady state and with $Q_{\mathrm{u}}$ constant, it was in [2] shown that for any step response, the state of optimal operation is left immediately if and only if $(u_{\mathrm{f}}, s) \in \mathcal{D}$; see Fig. 3. Consequently, as $(u_{\mathrm{f}}, s) \in \mathcal{S}$ the settler stays in optimal operation at least for a while. The sets $\mathcal{S}$ and $\mathcal{D}$ depend on $Q_{\mathrm{u}}$.

The situation during dynamic operation is similar but not identical. As the feed point moves out of $\mathcal{S}$ during dynamic operation, or $Q_{\mathrm{u}}(t)$ varies such that $\mathcal{S}(Q_{\mathrm{u}}(t))$ changes and excludes the feed point, the settler will immediately leave the state of optimal operation as the following theorem states. However, the converse is not true, as the second following theorem states.

As in the previous papers initial data are denoted with a zero index and refer to $t = 0-$, e.g. $u_{\mathrm{f}0} = u_{\mathrm{f}}(0-)$. The functions $u_{\mathrm{f}}(t)$, $Q_{\mathrm{u}}(t)$ and $s(t)$ are assumed to be piecewise monotone, piecewise $C^1$ and continuous from

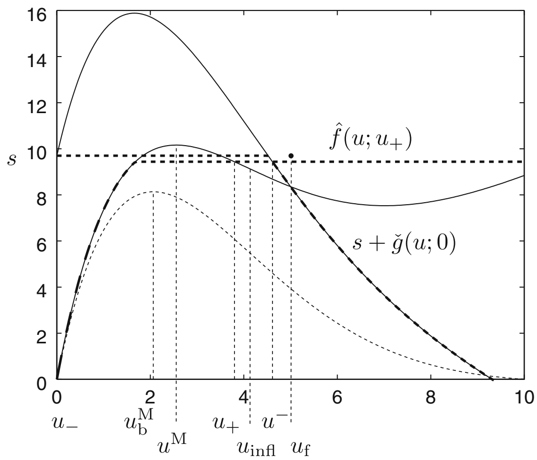


**Fig. 4** A case when optimal operation is not maintained despite $(u_f, s) \in \mathcal{S}$ and $Q_u < \bar{\bar{Q}}_u$. The concentration value of the maximum of the batch settling flux is denoted by $u_b^M \equiv u^M(Q_u = 0)$. Note that $u_+ = u_+(0)$ is the boundary value below the feed inlet at $t = 0-$ and $u^- = u^-(0)$ the new one above the feed inlet at $t = 0+$. Since $u^- > 0$ optimal operation is left

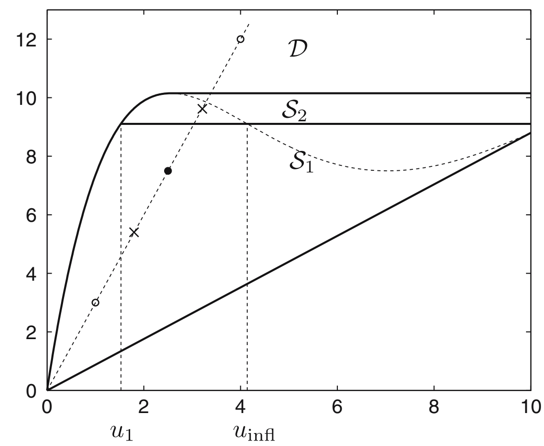


**Fig. 5** Operating chart as $Q_u = 2488\,\mathrm{m}^3/\mathrm{h}$ showing the regions $\mathcal{S} = \mathcal{S}_1 \cup \mathcal{S}_2$ and $\mathcal{D}$. Located on the dashed feed line $y = (Q_f/A)u$ are the feed points of two examples below; the crosses correspond to Example 1 (Figs. 6 and 8), and the circles to Example 2 (Figs. 7 and 9). The filled dot is the initial feed point $(u_{f0}, s_0) = (2.5, 7.5)$ in those examples. The concentration $u_1$ is used in the proof of Theorem 3.2

the right. For example, $u_0^M = u^M(Q_u(0-)) \neq u^M(Q_u(0))$ if $Q_u$ makes a step change at $t = 0$. We introduce the notation $u_b^M \equiv u^M(Q_u = 0)$ for the concentration value of the maximum of the batch settling flux (see Fig. 4).

**Theorem 3.1** *Given a settler in optimal operation at* $t = 0-$. *If* $(u_f(0), s(0)) \in \mathcal{D}(Q_u(0))$, *then the settler is not in optimal operation for small* $t > 0$.

*Proof* From the definition of optimal operation we have $u_-(0) = 0$ and $u_+(0) \in [0, u_{infl}]$. The statement follows by applying Condition Γ. We consider two cases within $\mathcal{D}(Q_u(0))$. If $(u_f(0), s(0)) \in \ell_4(Q_u(0)) \cup \mathcal{U}_2(Q_u(0))$, then $s(0) > f\left(u^M(Q_u(0))\right)$ and Condition Γ yields $u^+(0) > u_M(Q_u(0)) > u_{infl}$, which contradicts optimal operation. If $(u_f(0), s(0)) \notin \ell_4 \cup \mathcal{U}_2$, then—by considering the subcases $u_f(0) \lessgtr u^M(Q_u(0))$—one can conclude that the intersection of $\breve{g}(\cdot; 0) + s(0)$ and $\hat{f}(\cdot; u_+(0))$ occurs, in both subcases, at a flux value $\gamma(0) < s(0)$ and at a positive concentration, for which Condition Γ yields $u^-(0) > 0$. Hence, there is a non-zero concentration in the clarification zone and the settler is not in optimal operation. □

As examples of the two cases in the proof we refer to the step responses in [2]. For the first case, where $(u_f, s) \in \mathcal{D} \cap (\ell_4 \cup \mathcal{U}_2)$ (a small set in the right of the operating chart) and $u^+(0) > u_{infl}$, compare with Fig. 23 in [2], and for the second case, where $u^-(0) > 0$, Figs. 6, 13 (left), 17 (left), 29, 32 (left), 35 (left) in [2].

To maintain optimal operation it is thus necessary to have the feed point in $\mathcal{S}(Q_u(t))$ (and $Q_u(t) < \bar{\bar{Q}}_u$). However, this is not sufficient. There is the following exceptional case. Suppose $Q_u(t)$ is continuous at $t = 0$ and $u_+(0) \in (u^M, u_{infl})$; see Fig. 4. Then there is a plateau of $\hat{f}(\cdot; u_+(0))$ that lies below the local maximum point at $u^M$; $\hat{f}\left(u^M; u_+(0)\right) < f(u^M)$. Suppose also that the feed point lies above this plateau and in $\mathcal{S}$; $\hat{f}\left(u^M; u_+(0)\right) < s(0) \leq f(u^M)$. Then Condition Γ yields $u^-(0) > 0$ (cf. the second case in the proof of Theorem 3.1). There will be a transport of particles upwards in the clarification zone and optimal operation is left. Note that $f'(u_+(0)) < 0$.

Sufficient conditions for keeping optimal operation (at least for a while) are given in the following theorem, in which the four alternative prerequisites are introduced only to assure that the problem addressed in the previous paragraph does not occur. We define the following two disjoint subregions of $\mathcal{S}$; see Fig. 5:

$$\mathcal{S}_1(Q_u(t)) = \mathcal{S}(Q_u(t)) \cap \left\{(u, y) : y \leq f(u_{infl}; Q_u(t))\right\},$$
$$\mathcal{S}_2 = \mathcal{S} \setminus \mathcal{S}_1.$$

**Theorem 3.2** *Given a settler in optimal operation at* $t = 0-$. *Assume that* $Q_u(t) < \bar{\bar{Q}}_u$ *and* $(u_f(t), s(t)) \in \mathcal{S}(Q_u(t))$ *holds for* $t > 0$. *Assume also that one of the following holds:*

(a) $u(x,0) \in [0, u^M_{min}]$ *for* $0 < x < x_{sb}(0)$ *and* $s(t) \le f(u^M_{min})$ *for* $t > 0$, *where* $u^M_{min} \equiv \inf_{\tau > 0} u^M(Q_u(\tau))$;

(b) $u(x,0) \in \left[0, u^M(Q_u(0))\right]$ *for* $0 < x < x_{sb}(0)$ *and* $Q_u(t)$ *is non-decreasing for* $t > 0$;

(c) $u(x,0) \in [0, u^M_b]$ *for* $0 < x < x_{sb}(0)$ *and* $s(t) \le f(u^M_b)$ *for* $t > 0$;

(d) $(u_f(t), s(t)) \in \mathcal{S}_1(Q_u(t))$ *for* $t > 0$.

*Then the settler stays in optimal operation until the sludge blanket reaches the feed level or the bottom.*

*Remark* Each of the prerequisites (a)–(c) guarantees that all waves (characteristics and discontinuities) above the sludge blanket have positive speeds. In (d) there may be waves with negative speeds, however, they will disappear.

*Proof* Consider assumption (a). Since the concentrations above the SBL lie in $[0, u^M_{min}]$ the corresponding characteristics all have non-negative slope. Optimal operation implies that the boundary concentrations at the feed level satisfy $u_-(t) = 0$ and $u_+(t) \in [0, u^M_{min}]$ at $t = 0$. Given such values at any time point $t \ge 0$, the intersection of $\hat{f}(\cdot; u_+(t))$ and $\check{g}(\cdot; 0) + s(t)$ occurs in $[0, u^M_{min}]$ by the assumption $s(t) \le f(u^M_{min})$. By Condition $\Gamma$ this yields the boundary concentrations $u^-(t) = 0$ and $u^+(t) \in [0, u^M_{min}]$, which by the regularity assumptions hold for at least a small time interval. Hence, only waves with positive speeds are produced just below the feed level. They move down to the SBL where they define the boundary concentration above this discontinuity. By the well-known ordering principle for solutions of this type of equation, concentrations outside the interval $[0, u^M_{min}]$ cannot be created above the SBL. A similar situation holds below the SBL. At $t = 0$ the concentration lies in $(u_{infl}, u_{max}]$. For all such values of the boundary concentrations at the bottom, $u_D(t)$, formula (6) in [2] implies that $u^D(t) \in [u_M, u_{max}] \subset (u_{infl}, u_{max}]$. Then the jump and entropy conditions, together with the fact that the boundary concentrations above the SBL lie in $[0, u^M_{min}]$, imply that the concentrations just below the SBL lie in $[u^{M*}_{min}, u_{max}] \subset (u_{infl}, u_{max}]$. Consequently, the settler stays in optimal operation until the sludge blanket reaches either the feed level or the bottom. Consider assumption (b). This case can be treated similarly as in (a) with the following observations. Firstly, since $Q_u(t)$ is non-decreasing and $u^M(\cdot)$ is an increasing function, $u^M(Q_u(0)) = u^M_{min}$ holds. Hence the initial data satisfy the same condition as in (a). Secondly, the interval $[0, u^M_{min}]$ in the proof of (a) can be replaced by the $\left[0, u^M(Q_u(t))\right]$ for the following reasons. The length of this interval is non-decreasing and is an increasing part of $f(\cdot, Q_u(t))$. The assumption $(u_f(t), s(t)) \in \mathcal{S}(Q_u(t))$ always implies that $s(t) \le f\left(u^M(Q_u(t)), Q_u(t)\right)$, As in (a) Condition $\Gamma$ implies that only waves with positive speed are created just below the feed level. The monotonicity of $Q_u(t)$ implies that these waves always have positive speed and the proof can be continued as in (a). (c) follows directly from (a) since $u^M_b = u^M(0) \le u^M_{min}$ and $s(t) \le f(u^M_b) = f\left(u^M(0)\right) \le f\left(u^M(Q_u(t))\right)$, $\forall t$. Consider assumption (d). Optimal operation implies that $u_+(t) \in [0, u_{infl})$ for small $t > 0$. This implies that the plateau of $\hat{f}(\cdot; u_+(t))$ lies in the flux interval $\left(f(u_{infl}), f(u^M)\right]$, which is above $\mathcal{S}_1$. Since $s \le f(u_{infl})$, the plateau of $\check{g}(\cdot; 0) + s(t)$ lies on or below the level $s \le f(u_{infl})$. Hence the intersection of $\check{g}(\cdot; 0) + s(t)$ and $\hat{f}(\cdot; u_+(t))$ occurs on the graph of $f$ at a concentration in $[0, u_1]$, where $f(u_1) = f(u_{infl})$ and $u_1 < u_{infl}$, see Fig. 5, ($u_1$ is constant if $Q_u$ is constant, otherwise it depends continuously on $t$ at least for a small time interval). Condition $\Gamma$ implies that $u^-(t) = 0$ and $u^+(t) \le u_1(t)$ for small $t > 0$, and only new waves with positive speeds are created just below the feed level and with concentrations satisfying optimal operation. In particular, if there were 'problem' concentrations in $(u^M, u_{infl})$ below the feed level and above the SBL initially, a discontinuity would be created at the feed level having concentrations $\le u_1$ above it and concentrations in $(u^M, u_{infl})$ below it. By the jump condition such a discontinuity has a positive speed. As this reaches the SBL these initial 'problem' concentrations disappear. The situation is then as in case (a). □

As the feed point varies moderately and $Q_u$ is held constant, the following result is interesting, referring to one of the purposes of the settler; see Sect. 2.1.

**Corollary 3.1** *Given the assumptions in Theorem 3.2 with the following restrictions:* $u(x,0) = u_M$ *for* $x_{sb}(0) < x < D$ *and* $Q_u$ *is constant; then* $u_u$ *is constant until the SBL reaches the bottom.*

*Proof* The proof of the theorem gives that the possible concentrations above the sludge blanket are $[0, u^{\mathrm{M}}_{\min}] = [0, u^{\mathrm{M}}]$. The jump and entropy conditions imply that the only possible new concentrations that may be created just below the sludge blanket are $[u^{\mathrm{M}*}, u_{\mathrm{M}}]$. The characteristics corresponding to these concentrations have non-positive speed. Consequently, as long as the sludge blanket does not meet the bottom, there is an interval above the bottom, $\left(\sup_{\tau\in[0,t]} x_{\mathrm{sb}}(\tau), D\right)$, in which the concentration is constant $u_{\mathrm{M}}$. Formula (6) in [2] implies that the boundary concentration at the bottom is $u^D(t) = u_{\mathrm{M}}$ and the underflow concentration is constant $u_{\mathrm{u}} = f(u_{\mathrm{M}})/q_{\mathrm{u}}$ (mass conservation, cf. formula (8) in [2]). □

From [3, Table 2] we can conclude that a necessary condition for keeping optimal operation after a step input is that $(u_{\mathrm{f}}, s) \in P_1 \cup \Lambda_2 \cup \Lambda_{3\mathrm{a}}$; see Fig. 2. If, in addition, the SBL is not too close to the bottom (inequality (9) in [3] holds), optimal operation can be maintained. Furthermore, if the SBL meets the bottom, it was shown that the SBL can be restored within the thickening zone again after a finite time. Accordingly, a necessary condition for maintaining optimal operation during long time of dynamic operation is that

$$(u_{\mathrm{f}}(t), s(t)) \in P_1 \cup \Lambda_2 \cup \Lambda_{3\mathrm{a}}. \tag{2}$$

Hence, we only consider such cases in the numerical examples.

For the numerical simulations we use the data and batch-settling flux function shown in the caption of Fig. 1, and the numerical method in [54].

*Example 1* To demonstrate the dynamic behaviour we assume that the settler is in optimal operation initially with $(u_{\mathrm{f0}}, s_0) = (2.5\,\mathrm{kg/m^3}, 7.5\,\mathrm{kg/(m^2h)})$, see the filled dot in Fig. 5, and the corresponding $Q_{\mathrm{u0}} = L_1^{-1}(2.5, 7.5) = 2488\,\mathrm{m^3/h}$. The feed concentration is a periodic, piecewise constant function, with a period of 4 h, taking the alternating values 1.8 and $3.2\,\mathrm{kg/m^3}$. Assume that $Q_{\mathrm{f}}/A = 3\,\mathrm{m/h}$ is constant. Hence, $s(t)$ is piecewise constant taking the alternating values $3.1.8 = 5.4$ and $3.3.2 = 9.6\,\mathrm{kg/(m^2h)}$, see the crosses in Fig. 5. A simulation where $Q_{\mathrm{u}}(t) = Q_{\mathrm{u0}}$ is held constant is shown in Fig. 6. The underflow concentration is unchanged, cf. Corollary 3.1, and the SBL and mass vary periodically with constant mean values. Hence optimal operation is valid despite $(u_{\mathrm{f}}, s) \in \mathcal{S}_2$ half the time.

*Example 2* Let the initial data be the same as in Example 1 but let the amplitude of the periodic feed concentration alternate between 1 and $4\,\mathrm{kg/m^3}$ instead; see the circles in Fig. 5. The high load yields $(u_{\mathrm{f}}, s) = (4, 12) \in \mathcal{D}$. In accordance with Theorem 3.1, the simulation in Fig. 7 shows how optimal operation is left. At the end of the high-load intervals overflow occurs.

## 4 Manual control

Strategies for optimal control of step inputs are presented in [3]. We shall here generalize the situation and discuss and illustrate how such optimal control actions influence the dynamic behaviour when there is a series of step inputs as in Examples 1 and 2 above.

Initially, the settler is in optimal operation in steady state with $(u_{\mathrm{f0}}, s_0) \in \ell_2 \cup \ell_3$. At $t = 0$ there is a step change in the feed variables. A necessary condition for obtaining optimal operation in the corresponding new steady state is that $(u_{\mathrm{f}}, s) \in P_1 \cup \Lambda_2 \cup \Lambda_{3\mathrm{a}}$. For step changes in this region strategy DCL1 will in most cases imply that the settler stays in optimal operation. The only exception is when $(u_{\mathrm{f}}, s) \in \mathcal{D} \cap (P_1 \cup \Lambda_2 \cup \Lambda_{3\mathrm{a}})$ and the initial SBL lies close to the bottom, see [3, Sect. 7.5 and Fig. 31]. In any case, the location of the SBL in the new steady state is generally not the same as the initial one.

Consider a step input such that $s$ is decreased. Preventing an underloaded settler by lowering $Q_{\mathrm{u}}$ directly according to DCL1, implies that the mass leaving the settler per time unit through the underflow, $u_{\mathrm{u}}(t)Q_{\mathrm{u}}(t)$, jumps directly down to the same value as the fed mass, $u_{\mathrm{f}}(t)Q_{\mathrm{f}}(t) = As(t)$. The consequences are that the underflow concentration makes a step increase directly and then stays constant, the mass in the settler is unchanged and the SBL is stabilized, see [3, Sects. 6.2–6.3].

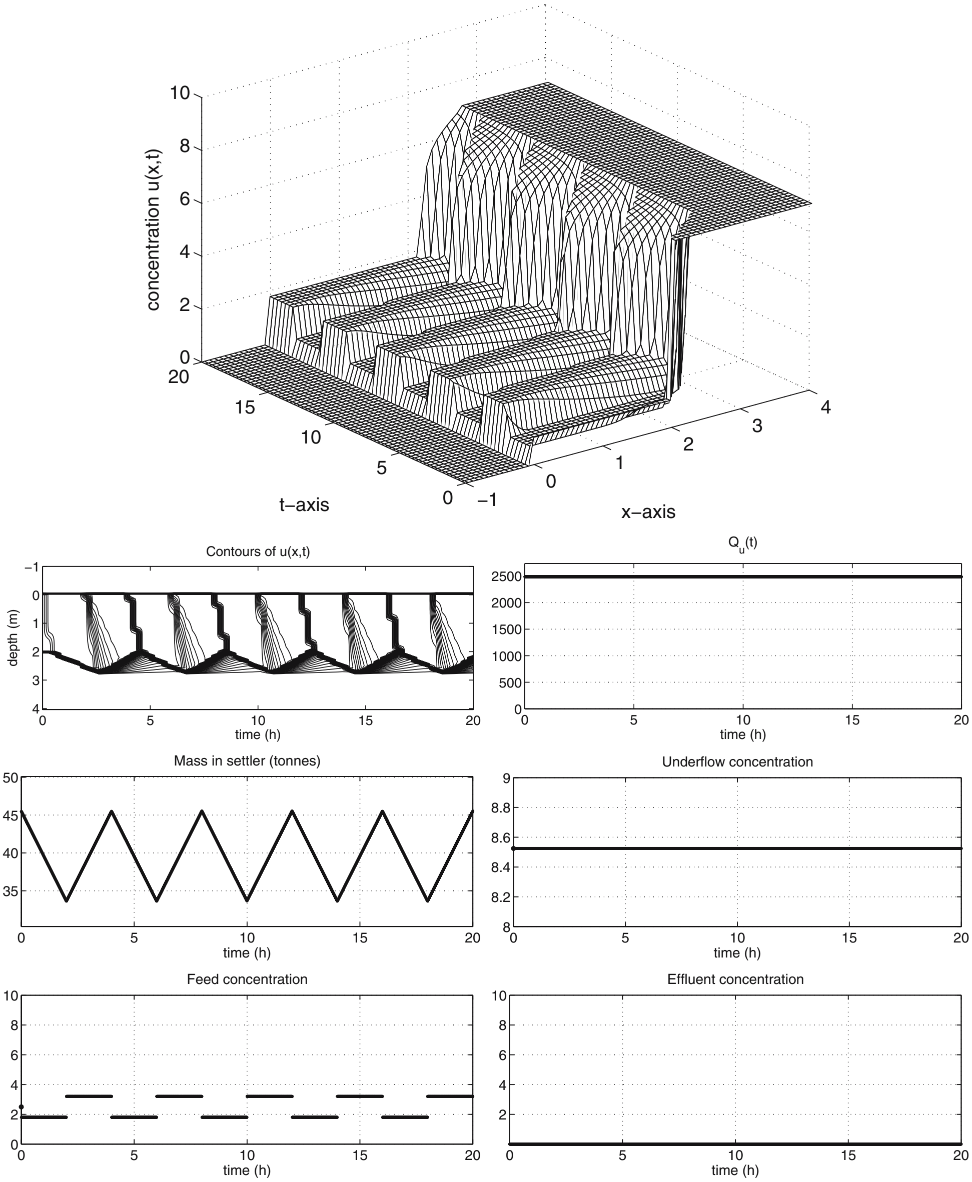


**Fig. 6** *Example 1*. A numerical simulation as the feed concentration is piecewise constant and periodic with the alternating values 1.8 and 3.2 kg/m$^3$. $Q_f(t) = 8482\,\mathrm{m}^3/\mathrm{h}$, $(u_{f0}, s_0) = (2.5, 7.5)$, $u_u(t) = u_{u0} = 8.52\,\mathrm{kg/m}^3$ and $Q_u(t) = Q_{u0} = L_1^{-1}(u_{f0}, s_0) = 2488\,\mathrm{m}^3/\mathrm{h}$

If the feed flux $s$ is increased in a step input, then DCL1 ($Q_u$ is increased) prevents an overloaded settler (see for example Fig. 16 in [3]). Below the SBL the concentration is constant $u_{M0}$ and the flux of these particles is (after the step change) greater than the incoming flux; $f(u_{M0}) > s$. This implies $u_u(t)Q_u = Af(u_M) > As = u_f(t)Q_f(t)$, that is, the mass leaving the settler is greater than the mass fed per unit time. Hence, the mass decreases and the new stationary SBL is either lower than the initial one, or it reaches the bottom during the transient.

These properties indicate that a direct-control strategy (DCL1) will imply that the SBL decreases, although optimal operation is maintained. We illustrate this with two examples.

*Example 1 (continued)* Applying DCL1 yields the simulation shown in Fig. 8. Let $Q_u^{\mathrm{low}}$ and $Q_u^{\mathrm{high}}$ denote the low and high values of $Q_u(t)$ corresponding to the low and high values of $u_f(t)$, respectively. Note that the upper limit for

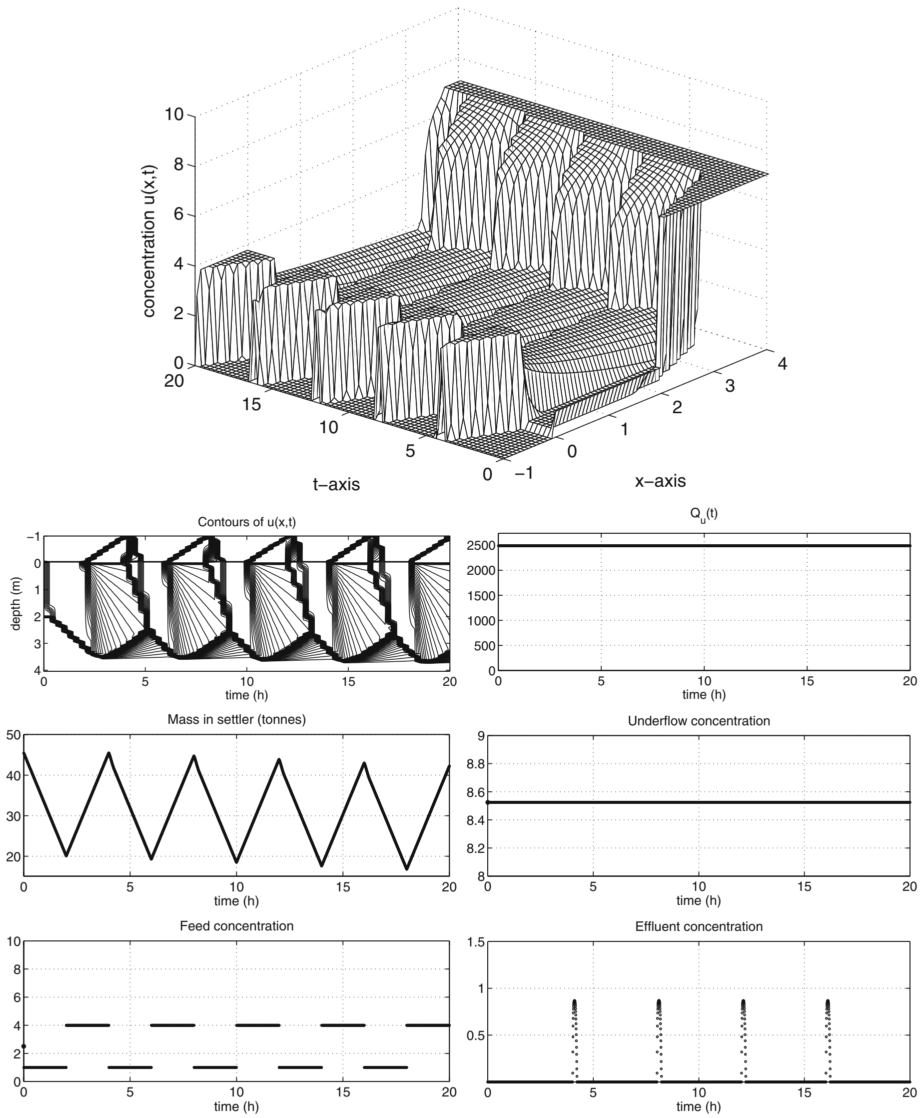


**Fig. 7** *Example 2.* A simulation where the alternating values of the periodic feed concentration are 1 and $4\,\mathrm{kg/m^3}$. This larger amplitude than in Example 1 implies overflow and a slightly declining SBL and mass, on an average. $Q_\mathrm{f}(t) = 8482$, $(u_\mathrm{f0}, s_0) = (2.5, 7.5)$, $u_\mathrm{u}(t) = u_\mathrm{u0} = 8.52$ and $Q_\mathrm{u}(t) = Q_\mathrm{u0} = L_1^{-1}(u_\mathrm{f0}, s_0) = 2488$

optimal operation is $\bar{\bar{Q}}_\mathrm{u} = 5159\,\mathrm{m^3/h}$. Figure 8 shows clearly that the SBL is declining and will eventually reach the bottom (after 100 h). Furthermore, the underflow concentration fluctuates. In this example no control at all (Fig. 6) is better than direct control (Fig. 8). The reason for the decreasing mass is that the mass leaving the settler on a four-hour time average, mean $(Q_\mathrm{f}(t)u_\mathrm{f}(t)) = \frac{1}{4}\int_0^4 Q_\mathrm{u}(t)u_\mathrm{u}(t)\,\mathrm{d}t$, is larger than the mass fed to the settler, mean $(Q_\mathrm{f}(t)u_\mathrm{f}(t))$. We also note that the average value of the control parameter, $(Q_\mathrm{u}^\mathrm{low} + Q_\mathrm{u}^\mathrm{high})/2 = 2535$, is larger than the value $Q_\mathrm{u0} = L_1^{-1}(2.5, 7.5) = 2488$, which corresponds to the initial stationary optimal-operation state.

*Example 2 (continued)* As the feed point jumps upwards in the operating chart to $(u_\mathrm{f}, s) = (4, 12) \in \mathcal{D}$, there will be a rising discontinuity in the clarification zone (cf. Theorem 3.1) unless the control parameter is increased. Strategy DCL1 implies that $Q_\mathrm{u}^\mathrm{low} = L_1^{-1}(1, 3) = 875$ and $Q_\mathrm{u}^\mathrm{high} = L_1^{-1}(4, 12) = 4563$, of which the average,

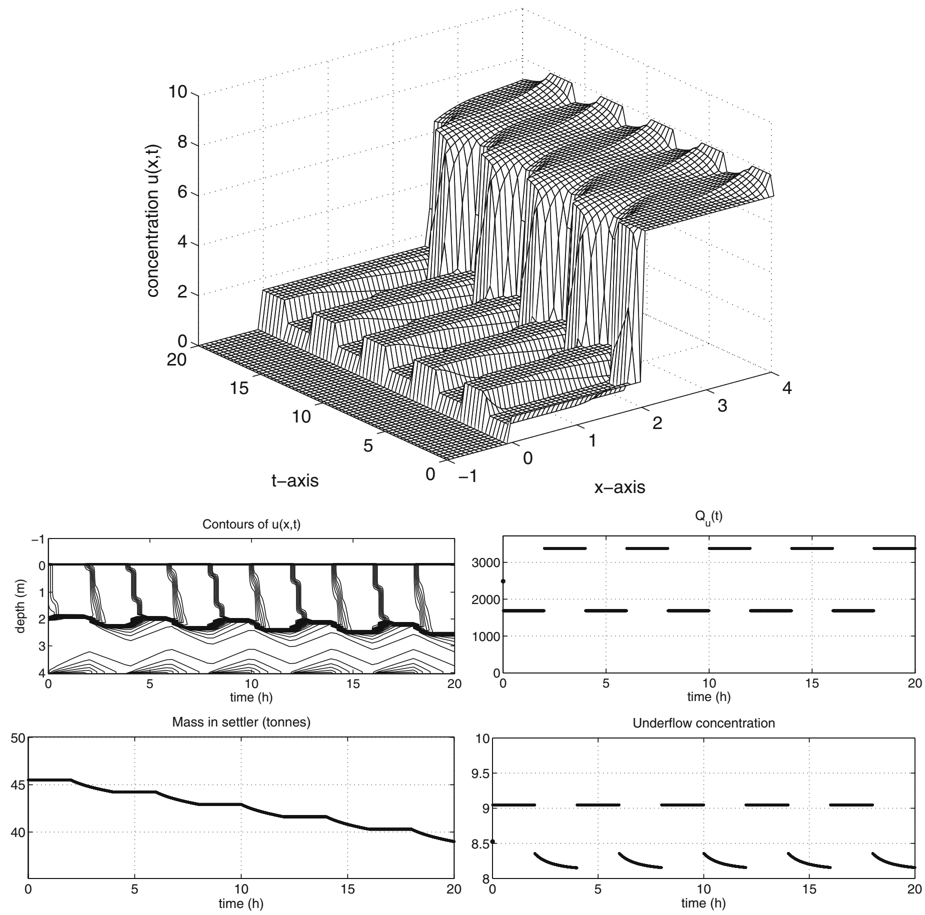


**Fig. 8** *Example 1 (continued).* A simulation using the same initial data and the same feed concentration as in Fig. 6. DCL1 is applied. The two values of $Q_\mathrm{u}(t)$ are $Q_\mathrm{u}^\mathrm{low} = L_1^{-1}(1.8, 5.4) = 1688$ and $Q_\mathrm{u}^\mathrm{high} = L_1^{-1}(3.2, 9.6) = 3382$. Note that the average value of $Q_\mathrm{u}$ is higher than the initial one, which corresponds to a stationary optimal-operation state. Continued simulation shows that the SBL reaches the bottom after 100 h

2719, is substantially greater than $Q_{\mathrm{u}0} = L_1^{-1}(2.5, 7.5) = 2488$. The simulation, shown in Fig. 9, reveal a similar behaviour as in Fig. 8 with a declining SBL and mass.

Therefore, we demonstrate a modified strategy with the time average of $Q_\mathrm{u}(t)$ equal to $Q_{\mathrm{u}0}$. During the intervals when $(u_\mathrm{f}, s) = (4, 12)$, we choose $Q_\mathrm{u}^\mathrm{high} = L_3^{-1}(4, 12) = 4335$, which is the lowest possible value of $Q_\mathrm{u}$ satisfying $(u_\mathrm{f}, s) \in \mathcal{S}(Q_\mathrm{u}^\mathrm{high})$. With the lower value set to $Q_\mathrm{u}^\mathrm{low} = 2Q_{\mathrm{u}0} - Q_\mathrm{u}^\mathrm{high} = 2 \cdot 2488 - 4335 = 640$ we get the simulation in Fig. 10. The mass is now slightly increasing on a four-hour average. In fact, the mass increases with the rate mean $(Q_\mathrm{f}(t)u_\mathrm{f}(t) - Q_\mathrm{u}(t)u_\mathrm{u}(t)) = 155$ kg/h. The reason is of course the nonlinear dependence of $u_\mathrm{u}(t)$ on $Q_\mathrm{u}(t)$. Thus, to maintain optimal operation during long times for a periodically varying feed point with mean value corresponding to a stationary optimal-operation solution, it is not sufficient to choose the control variable with mean value according to a stationary solution. However, with a small manual adjustment of the latter strategy—decrease $Q_\mathrm{u}^\mathrm{min}$ slightly—the process can be controlled satisfactorily.

## 5 Conclusions

In this series of papers, the nonlinear behaviour has been classified by means of operating charts, which are concentration-flux diagrams in which the location of the feed point yields qualitative and quantitative information of the

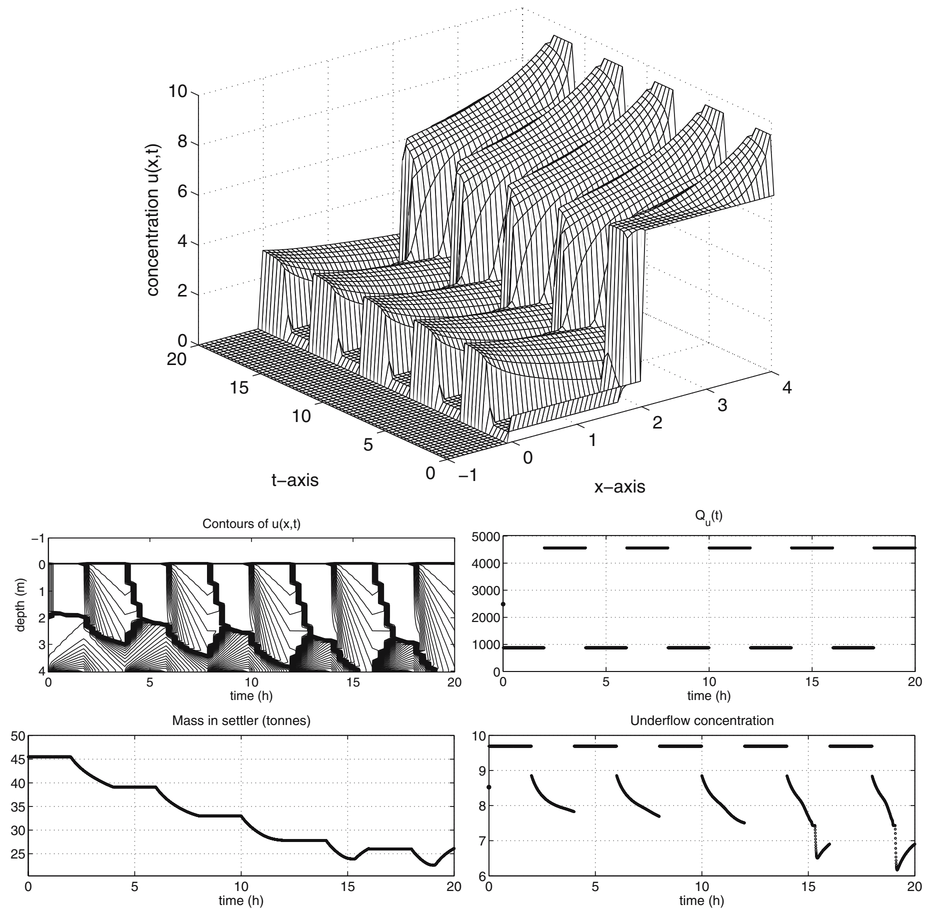


**Fig. 9** *Example 2 (continued)*. A simulation using the same initial data and the same feed concentration as in Fig. 6. DCL1 is applied. The two values of $Q_{\mathrm{u}}(t)$ are $Q_{\mathrm{u}}^{\mathrm{low}} = L_1^{-1}(1, 3) = 875$ and $Q_{\mathrm{u}}^{\mathrm{high}} = L_1^{-1}(4, 12) = 4563$. The SBL and mass are declining and optimal operation is left after 15 h

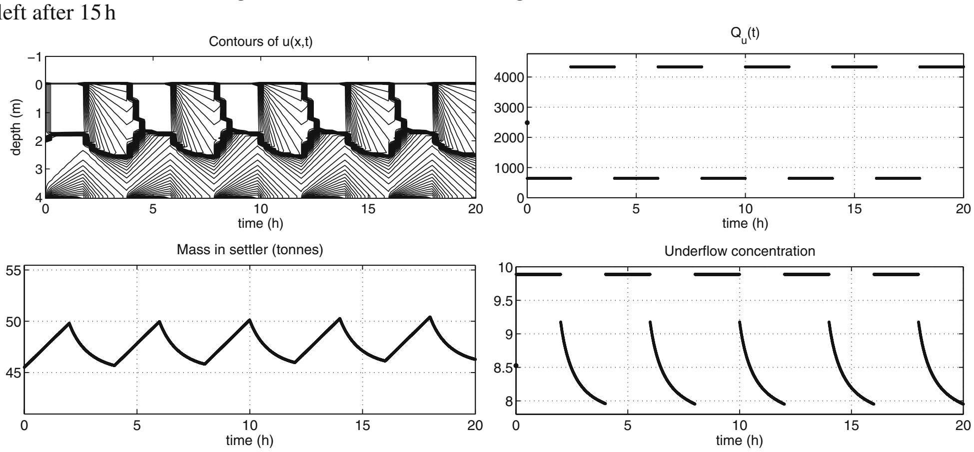


**Fig. 10** *Example 2 (continued)*. A control strategy where $Q_{\mathrm{u}}^{\mathrm{high}}$ is chosen such that $(u_{\mathrm{f}}, s) \in \mathcal{S}(Q_{\mathrm{u}}^{\mathrm{high}})$ during the intervals of high feed concentration, and $Q_{\mathrm{u}}^{\mathrm{low}}$ such that $\frac{1}{2}(Q_{\mathrm{u}}^{\mathrm{low}} + Q_{\mathrm{u}}^{\mathrm{high}}) = Q_{\mathrm{u}0}$. Note that the mass is slightly increasing on a four-hour average

process. As the feed point varies with time it may move from one region to another, which results in a qualitative change in the behaviour of the process.

One division of the concentration-flux diagram depends only on the batch settling flux function; see the operating chart in Fig. 2 (right). A necessary condition for maintaining optimal operation during long time of dynamic operation is (2). This condition is not satisfied if the feed concentration or the ratio $Q_{\mathrm{f}}/A$ is too large. Normally, the feed concentration is low since the purpose of the device is to thicken the suspension. With the given batch settling flux function, feed concentrations above the inflection point, $u_{\mathrm{infl}} = 4.1\,\mathrm{kg/m^3}$, implies that the thickening factor, the ratio $u_{\mathrm{u}}/u_{\mathrm{f}}$ for a critically loaded settler, is less than 2, see [1, Fig. 12]. Hence, it is reasonable that $u_{\mathrm{f}} < u_{\mathrm{infl}}$ holds normally. If $u_{\mathrm{f}}$ is low and still $(u_{\mathrm{f}}, s) \notin P_1 \cup \Lambda_2 \cup \Lambda_{3\mathrm{a}}$, then $Q_{\mathrm{f}}/A$ is large. Then the cross-sectional area is too small—the plant is underdimensioned. However, if $(u_{\mathrm{f}}, s) \notin P_1 \cup \Lambda_2 \cup \Lambda_{3\mathrm{a}}$ occurs, $Q_{\mathrm{u}}$ has to be increased sufficiently (even above $\bar{\bar{Q}}_{\mathrm{u}}$) so that overflow does not occur. Then the SBL will disappear from the thickening zone; cf. [3], where the control of step responses cover all cases.

Other divisions of the operating chart depend on the flux function in the thickening zone, which depends on the control variable; see Figs. 2 (left), 3, and 5. Accordingly, even for a constant feed point, the behaviour of the process may change substantially as the control variable changes.

The limitations of the control variable to maintain optimal operation have been established in Sect. 3. Consider the operating chart in Fig. 3. The feed point may be located in the region above the line $y = q_{\mathrm{u}} u$. This region can be divided into two disjoint regions, the safe, $\mathcal{S}$, and the dangerous, $\mathcal{D}$, which both depend on $Q_{\mathrm{u}}$. For step responses from optimal operation in steady state, the following nice equivalence holds: the state of optimal operation is left immediately if and only if $(u_{\mathrm{f}}, s) \in \mathcal{D}$. Consequently, as $(u_{\mathrm{f}}, s) \in \mathcal{S}$ the settler stays in optimal operation at least for a while.

For a general dynamic solution the situation is similar but not identical. Theorem 3.1 states that optimal operation is left immediately if $(u_{\mathrm{f}}, s) \in \mathcal{D}$. From the proof we can infer two different situations. One occurs only for high values of the feed concentration and is therefore probably not of interest for the applications. The other situation is the interesting one in practice, when the feed concentration is not too high. Then optimal operation is left because of an upflow of particles in the clarification zone.

During dynamic operation, optimal operation can be left even if $(u_{\mathrm{f}}, s) \in \mathcal{S}$. A sufficient condition for maintaining optimal operation, (at least for a while) which does not depend on the concentration distribution, is that $(u_{\mathrm{f}}, s) \in \mathcal{S}_1$, see Theorem 3.2 and Fig. 5. Thus, a theoretically safe lower bound $Q_{\mathrm{u}}^{\min}(t)$ of the control variable is the minimal value that satisfies

$$(u_{\mathrm{f}}(t), s(t)) \in \mathcal{S}_1 \left( Q_{\mathrm{u}}^{\min}(t) \right) .$$

In many cases this means that $(u_{\mathrm{f}}, s)$ lies on the horizontal boundary between $\mathcal{S}_1$ and $\mathcal{S}_2$, which means that $s(t) = f\left(u_{\mathrm{infl}}, Q_{\mathrm{u}}^{\min}(t)\right)$. A high value of $s$ implies a high value of $Q_{\mathrm{u}}^{\min}$, which may imply a fast declining SBL and a low underflow concentration. Furthermore, in a wastewater treatment plant, most of the underflow is returned to a biological reactor before the settler, and high flow values may be disadvantageous.

For $(u_{\mathrm{f}}, s) \in \mathcal{S}_2$ (see Fig. 5) it is only exceptionally that optimal operation is left. Thus, a less restrictive condition, which we recommend, is to define $Q_{\mathrm{u}}^{\min}(t)$ such that

$$(u_{\mathrm{f}}(t), s(t)) \in \mathcal{S} \left( Q_{\mathrm{u}}^{\min}(t) \right) \tag{3}$$

holds. This implies a lower value of $Q_{\mathrm{u}}^{\min}(t)$. If the location of the feed point is such that $(u_{\mathrm{f}}(t), s(t)) \in \mathcal{S}(0)$, then $Q_{\mathrm{u}}^{\min}(t)$ can be set to a small positive value. (We have assumed that $Q_{\mathrm{u}}(t) > 0$, otherwise $u_{\mathrm{u}}(t)$ is undefined.) Otherwise, we define $Q_{\mathrm{u}}^{\min}(t) = L_3^{-1}\left(u_{\mathrm{f}}(t), s(t)\right)$, which means that the feed point lies on the upper boundary of $\mathcal{S}$; see Fig. 5. The exceptional problematic case that may occur when $(u_{\mathrm{f}}, s) \in \mathcal{S}_2$ is when the concentration happens to be rather high (in the interval $(u^{\mathrm{M}}, u_{\mathrm{infl}})$) just below the feed level. This is believed to occur only rarely, and if it occurs, we may allow some particles in the lower part of the clarification zone during a limited time period. The advantage of a lower value of $Q_{\mathrm{u}}^{\min}$, which is to reduce the risk for the SBL to reach the bottom, is thus probably more important in the application.

An upper bound on the control variable is $\bar{\bar{Q}}_{\mathrm{u}}$ by the definition of optimal operation. If a constraint of a control objective is that the underflow concentration should lie above a given lower bound, then this can be guaranteed by an upper bound on the control variable, see [3, Theorem 4.1]. Together with the lower bound defined above, we have thus defined a time-dependent interval in which the control variable must stay to maintain optimal operation.

The theoretical results and discussions have been exemplified by numerical simulations. We have used the control strategy DCL1 (direct control with respect to stationary optimal operation), which is the main part of the optimal control strategies for step inputs in [3], and the above-mentioned bounds of the control variable. Although the process can be controlled, the following nonlinear behaviour makes it difficult to define the exact appropriate values of the control variable: To maintain optimal operation during long times for a periodically varying feed point with mean value corresponding to a stationary optimal-operation solution, it is not sufficient to choose the control variable with mean value according to a stationary solution.

In Example 1, with a moderate amplitude of the oscillating feed point, we have seen that no control at all (Fig. 6) is in the long run better than DCL1 (Fig. 8). It is true that the oscillation of the SBL has a smaller amplitude with DCL1, but it declines slowly and will reach the bottom.

In Example 2 the amplitude of the oscillating feed point is so high that overflow occurs without any control. Strategy DCL1 prevents overflow, but results in a rather fast declining SBL. A modified strategy with the lowest possible control variable satisfying (3), during the intervals of high load, yields a much better control; see Fig. 9. The slowly, on an average, declining SBL can be adjusted by decreasing the control variable further during the intervals of low load. In this way the process can be controlled satisfying control objectives that requires that optimal operation is maintained and that the average SBL is kept in the middle of the thickening zone.

**Acknowledgement** I am grateful to Dr Ulf Jeppsson, Lund University, for his comments on the manuscript. This work has been supported by the Swedish Research Council (Vetenskapsrådet), project 621-2005-3873.

## References

1. Diehl S (2001) Operating charts for continuous sedimentation I: control of steady states. J Eng Math 41:117–144
2. Diehl S (2005) Operating charts for continuous sedimentation II: step responses. J Eng Math 53:139–185
3. Diehl S (2006) Operating charts for continuous sedimentation III: control of step inputs. J Eng Math 54:225–259
4. Diehl S (1995) On scalar conservation laws with point source and discontinuous flux function. SIAM J Math Anal 26(6):1425–1451
5. Diehl S (1996) A conservation law with point source and discontinuous flux function modelling continuous sedimentation. SIAM J Appl Math 56(2):388–419
6. Bürger R, Karlsen KH, Klingenberg C, Risebro NH (2003) A front tracking approach to a model of continuous sedimentation in ideal clarifier-thickener units. Nonl Anal Real World Appl 4:457–481
7. Bürger R, Karlsen KH, Risebro NH, Towers JD (2004) Well-posedness in $BV_t$ and convergence of a difference scheme for continuous sedimentation in ideal clarifier-thickener units. Numer Math 97:25–65
8. Karlsen KH, Towers JD (2004) Convergence of the Lax-Friedrichs scheme and stability for conservation laws with a discontinuous space-time dependent flux. Chinese Ann Math Ser B 25(3):287–318
9. Kynch GJ (1952) A theory of sedimentation. Trans Faraday Soc 48:166–176
10. Keinath TM, Ryckman M, Dana C, Hofer D (1977) Activated sludge–unified system design and operation. J Envir Eng Div ASCE 103(EE5):829–849
11. Laquidara VD, Keinath TM (1983) Mechanism of clarification failure. J Water Pollut Control Fed 55(1):54–57
12. Keinath TM (1985) Operational dynamics and control of secondary clarifiers. J Water Pollut Control Fed 57(7):770–776
13. Bürger R, Karlsen KH, Towers JD (2005) A model of continuous sedimentation of flocculated suspensions in clarifier-thickener units. SIAM J Appl Math 65:882–940
14. Karlsen KH, Risebro NH, Towers JD (2002) Upwind difference approximations for degenerate parabolic convection-diffusion equations with a discontinuous coefficient. IMA J Numer Anal 22:623–664
15. Karlsen KH, Risebro NH, Towers JD (2003) $L^1$ stability for entropy solutions of nonlinear degenerate parabolic convection-diffusion equations with discontinuous coefficients. Skr K Nor Vidensk Selsk 3:49 pp
16. Stehfest H (1984) An operational dynamic model of the final clarifier. Trans Inst Meas Control 6(3):160–164
17. Diehl S, Sparr G, Olsson G (1990) Analytical and numerical description of the settling process in the activated sludge operation. In: Briggs R (ed) Instrumentation, control and automation of water and wastewater treatment and transport systems. Pergamon Press, IAWPRC, pp 471–478
18. Bustos MC, Paiva F, Wendland W (1990) Control of continuous sedimentation as an initial and boundary value problem. Math Methods Appl Sci 12:533–548

19. Barton NG, Li C-H, Spencer J (1992) Control of a surface of discontinuity in continuous thickeners. J Austral Math Soc Ser B 33:269–289
20. Chancelier J-Ph, Cohen de Lara M, Pacard F (1994) Analysis of a conservation PDE with discontinuous flux: a model of settler. SIAM J Appl Math 54(4):954–995
21. Chancelier J-Ph, Cohen de Lara M, Joannis C, Pacard F (1997) New insight in dynamic modelling of a secondary settler—II. Dynamical analysis. Water Res 31(8):1857–1866
22. Diehl S (1997) Dynamic and steady-state behaviour of continuous sedimentation. SIAM J Appl Math 57(4):991–1018
23. Attir U, Denn MM (1978) Dynamics and control of the activated sludge wastewater process. AIChE J 24:693–698
24. Thompson D, Chapmand DT, Murphy KL (1989) Step feed control to minimize solids loss during storm flows. Res J Water Pollut Control Fed 61(11–12):1658–1665
25. Johnston RRM, Simic K (1991) Improving thickener operation and control by means of a validated model. Minerals Eng 4:695–705
26. Couillard D, Zhu S (1992) Control strategy for the activated sludge process under shock loading. Water Res 26:649–655
27. Kabouris JC, Georgakakos AP, Camara A (1992) Optimal control of the activated sludge process: effect of sludge storage. Water Res 26:507–517
28. Balslev P, Nickelsen C, Lynggaard-Jensen A (1994) On-line flux-theory based control of secondary clarifiers. Water Sci Technol 30(2):209–218
29. Grijspeerdt K, Verstraete W (1996) A sensor for the secondary clarifier based on image analysis. Water Sci Technol 33(1):61–70
30. Bergh S-G, Olsson G (1996) Knowledge based diagnosis of solids-liquid separation problems. Water Sci Technol 33:219–226
31. Kim Y, Pipes WO (1996) Solids routing in an activated sludge process during hydraulic overloads. Water Sci Technol 34(3–4):9–16
32. Nyberg U, Andersson B, Aspegren H (1996) Real time control for minimizing effluent concentrations during storm water events. Water Sci Technol 34:127–134
33. Sidrak YL (1997) Control of the thickener operation in alumina production. Control Eng Practice 5:1417–1426
34. Kim Y, Pipes WO, Chung P-G (1998) Control of activated sludge bulking by operating clarifiers in a series. Water Sci Technol 38(8–9):1–8
35. Dauphin S, Joannis C, Deguin A, Bridoux G, Ruban G, Aumond M (1998) Influent flow control to increase the pollution load treated during rainy periods. Water Sci Technol 37(12):131–139
36. Georgieva PG, FeyoDe Azevedo S. (1999) Robust control design of an activated sludge process. Int J Robust Nonlinear Control 9:949–967
37. Schoenbrunn F, Toronto T (1999) Advanced thickener control. In: Advanced process control applications for industry workshop. IEEE Industry Applications Society, pp 83–86
38. Vanderhasselt A, De Clercq B, Vanderhaegen B, Vanrolleghem P, Verstraete W (1999) On-line control of polymer addition to prevent massive sludge washout. J Env Eng 125:1014–1021
39. Charef A, Ghauch A, Martin-Bouyer M (2000) An adaptive and predictive control strategy for an activated sludge process. Bioprocess Biosyst Eng 23:529–534
40. Georgieva P, Ilchmann A (2001) Adaptive lambda-tracking control of activated sludge processes. Int J Control 12:1247–1259
41. Ito H A dissipative approach to control of biological wastewater treatment plants based on entire nonlinear process models. In: Proceedings of the 2004 American control conference, vol 6. IEEE (2004) pp 5489–5495
42. Olsson G, Nielsen MK, Yuan Z, Lynggaard-Jensen A, Steyer J-P Instrumentation, control and automation in wastewater systems. Intl Water Assn (2005)
43. Jeppsson U, Rosen C, Alex J, Copp J, Gernaey KV, Pons M-N, Vanrolleghem PA (2006) Towards a benchmark simulation model for plant-wide control strategy performance evaluation of WWTPs.. Water Sci Technol 53:287–295
44. Attir U, Denn MM, Petty CA (1977) Dynamic simulation of continuous sedimentation. AIChE Symp Ser No 167 73:49–54
45. Lumley DJ, Balmér P, Adamsson J (1988) Investigations of secondary settling at a large treatment plant. Water Sci Technol 20:133–142
46. Koehne M, Hoen K, Schuhen M (1995) Modelling and simulation of final clarifiers in wastewater treatment plants. Math Comput Simul 39(5–6):609–616
47. Göhle F, Finnson B, Hultman B (1996) Dynamic simulation of sludge blanket movements in a full-scale rectangular sedimentation basin. Water Sci Technol 33(1):89–99
48. Charmot-Charbonnel M-L, Ripoche G, Roche N, Prost C (1999) Modeling and simulation of activated sludge process with cyclic feeding for treatment of highly loaded wastewater. Chem Eng Tech 22:50–56
49. Manning WT, Garrett MT, Malina JF (1999) Sludge blanket response to storm surge in an activated-sludge clarifier. Water Environ Res 71:432–442
50. Wilén B-M, Lumley D, Nordqvist A (2004) Dynamics in maximal settling capacity in an activated sludge treatment plant with highly loaded secondary settlers. Water Sci Technol 50:187–194
51. De Clercq J, Devisscher M, Boonen I, Defrancq J, Vanrolleghem PA (2005) Analysis and simulation of the sludge profile dynamics in a full-scale clarifier. J Chem Technol Biotechnol 80:523–530
52. Wilén B-M, Lumley D, Mattsson A, Mino T (2006) Rain events and their effect on effluent quality studied at a full scale activated sludge treatment plant. Water Sci Technol 54:201–208
53. Diehl S, A regulator for continuous sedimentation in ideal clarifier-thickener units. Accepted for publication J Eng Math (2007)
54. Diehl S, Jeppsson U (1998) A model of the settler coupled to the biological reactor. Water Res 32(2):331–342